EVAPORATION CHARACTERISTICS AND EFFICIENT WORKING AREA OF MULTI-STAGE HIGH PRESSURE AND TEMPERATURE REDUCING VALVE

by

***Li-Hua CAO*[a], *He-Yong SI*[a*], *En-Fu DONG*[b], *Zhan-Zhou WANG*[a], *Huan-Huan LUO*[b], *Gui-Ping ZHOU*[b], *and Nan WU*[b]**

[a] School of Energy and Power Engineering, Northeast Electric Power University, Jilin, China
[b] State Grid Liaoning Electric Power Supply CO., LTD, Shenyang, China

Original scientific paper
https://doi.org/10.2298/TSCI200719162C

A well understanding on the evaporation characteristics and efficient working area of multi-stage high pressure and temperature reducing valve (MSHPTRV) is important for improving the performance and safety of MSHPTRV. The water spraying and evaporation model are integrated into the flow model of MSHPTRV. Compared with the experimental data, the model can show the thermal process well. The flow characteristics and interaction between steam and droplets are presented. On this basis, the increase rate of entropy, S_{dis}, is adopted to analyze the thermodynamic loss and innovatively determine the efficient working area of MSHPTRV. The results show that the pressure reducing effect of the second orifice plate is prominent, which accounts for 41.6% of the total pressure drop. The "steam-water layer" is formed at the boundary of steam and water. At the inlet of second orifice plate, the maximum S_{dis} is 0.782, and the downstream of second orifice plate is the efficient working area of MSHPTRV. The length of evaporation section increases with the droplets diameter significantly.

Key words: *MSHPTRV, evaporation model, water spraying, flow characteristics, increase rate of entropy*

Introduction

Steam energy can be regulated reasonably by MSHPTRV via reducing the steam pressure and temperature [1]. It produces qualified steam by throttling, diffusing and water spraying [2, 3]. The complex internal structure [4], two-phase flow of vapor and water will cause the high flow velocity as well as the severe variations of temperature and pressure [5]. These factors will seriously affect the efficiency and safety of the unit. Therefore, deeply understanding evaporation characteristics and efficient working area of MSHPTRV is essential for improving the performance [6].

There are many researches on various valves, which include the electromagnetic valves, pressure relief valves (PRV), and so on. Valve motion and pressure pulsation have the great influence on the thermodynamic performance of reciprocating compressors [7]. The valve regulation affects the efficiency of the whole system [8]. At present, the performance and safety of multi-stage high pressure reducing valve (MSHPRV) without temperature reducing (neglecting the water spraying) are usually investigated. Due to the difficulty in exper-

* Corresponding author, e-mail: ssiheyong0927@163.com

imental study of MSHPRV, the RNG k-ε model combining with compressible gas in CFD was established to simulate Mach number. The results show that the pressure ratio influences energy loss greatly. Furthermore, the flow field characteristics of DN80 pressure reducing valve under different inlet pressure and opening degrees were analyzed by [9]. The pressure reducing effect of MSHPRV can be improved with the increasing of valve opening degree [10]. For contra-push check valve, Xu *et al.* [11] conducted a sensitivity analysis of structural parameters. The influence of structural parameters on pressure induced force was studied. The RNG k-ε model was also proved to be more accurate for describing the flow field. But the analysis of flow characteristics and work efficiency of the valve were less. To investigate the pressure control performance of solenoid valve, Li *et al.* [12] simulated the cases of different pressure drops by mesh deformation. The results show that valve opening time can influence the mean control pressure. The temperature and pressure characteristics under different valve openings were presented and the application of MSHPRV in hydrogen refueling station was validated [13]. Zhang *et al.* [14] modeled the dynamic performance of the opening and closing of PRV by CFD. Analysis from flow field, the throttling components of high pressure reducing valve have great effects on the control performances. So the angle of throttling components, orifice plate thickness, plate number and diameter of plate holes in MSHPRV were studied in [15]. But it is difficult to describe the thermodynamic characteristics of fluid-flow through the pressure and velocity. In terms of valve safety, the flow forces and energy loss in a flapper-nozzle pilot valve under different clearances were studied, and the performance of the valve was evaluated. The larger flapper makes the lateral force increased 1.5-13.6% in drag direction and 1.5-10.2% in lift direction. Meanwhile, both experimental and numerical results show that the energy loss increases with inlet pressure, which proves the reliability of the simulation [16]. To simulate the fluid-structure interaction in non-returning valves, a 3-D unsteady model was established to compare with 2-D model, which indicates that the 3-D unsteady model can provide a more accurate flow field. It shows that the fluid-structure interaction makes exhausting valve tapped severely in forward stroke, and the aspirating valve has better sealing characteristics in initial backward stroke [17]. The analysis of transient thermal behaviors was acted on the basis of transient turbulent flow simulation and turbine valve experiment. It indicates that the second separated flow causes non-uniform heat transfer [18]. Benefiting from the advantages of fluid-structure coupling and structural mechanics, scholars carried out the failure analysis of valve body and predicted fatigue life. The von-Mises stresses caused by common factors, such as cooled steam, internal pressure were studied. Through the analysis of equipment and structural mechanical calculation, it was found that the expansion and contraction are the major factors for fatigue [19]. Chen *et al.* [20] proposed a new MSHPRV which can achieve multi-stage pressure reducing processes. The lower noise and energy consumption of the valve were achieved. Combined with the fluid-structure coupling model of proposed MSHPRV, the mathematical model of MSHPRV was established to study the thermo-mechanical stress [21]. The best strength of MSHPRV is obtained by optimizing geometrical factors [22]. The above researches studied the pressure reducing process of MSHPRV without considering the process of water spraying. In the vapor-liquid two-phase flow, Boccardi *et al.* [23] found two-phase discharge coefficient much higher than the vapor coefficient through a steam/water flashing experiment, and a new correlation for the discharge coefficient as a function of the main operating parameters was proposed. Schmidt [24] proposed partial non-equilibrium HNE-DS method to standardize all sizing procedures by an appropriate nozzle flow model and to enlarge the application range of the standards to two-phase flow. The MSHPTRV usually has a water spraying process to reduce temperature.

Namely, MSHPTRV reduces pressure and temperature at the same time. The two-phase flow and the water evaporation are the main factors for causing the complexity of the internal flow field. So studying the process of pressure reducing without water spraying is not applicable to MSHPTRV. The flow characteristics of MSHPTRV are different with MSHPRV because of different steam parameters. In the study of fluid-structure coupling model, the great variation of temperature caused by water flash spraying also affects the fatigue of valve [25].

In conclusion, it is necessary to further study the internal flow field of MSHPTRV with water spraying. In this study, the water spraying and evaporation model verified by experiment are innovatively integrated into MSHPTRV, in which the higher pressure and temperature 16.67 MPa/538 °C (main steam parameters of 300 MW unit) are adopted to obtain the actual thermodynamic process. Finally, the evaporation and flow characteristics of MSHPTRV are analyzed. And the increase rate of entropy, S_{dis}, is adopted to analyze the thermodynamic loss and the efficient working area of MSHPTRV.

Numerical method

Geometrical model

A C1Z604-0 MSHPTRV of bypass heating system is established by ANSYS Workbench. The structural parameters and physical model are shown in fig. 1. The MSHPTRV consists of the throttle orifice plates and nozzle of water spraying.

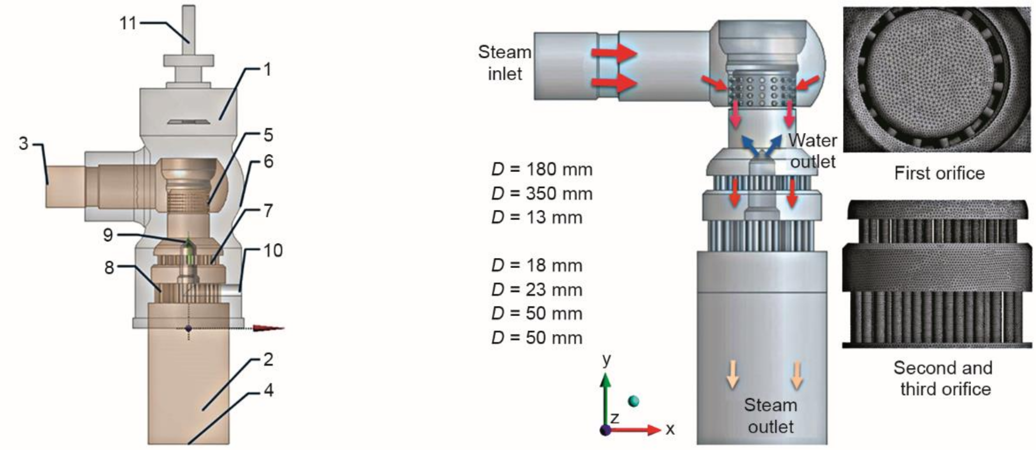

Figure 1. The MSHPTRV model; *1 – valve body, 2 – flow fields, 3 – steam inlet, 4 – steam outlet, 5 – first orifice, 6 – support ring, 7 – second orifice, 8 – third orifice, 9 – water outlet, 10 – water inlet, and 11 – valve stem*

The first throttle orifice plate is the valve core to regulate the steam flow rate. The high-parameter steam will flow into MSHPTRV from pipeline, and the steam flows through the first throttle orifice plate, the cooling water supplied by feed pump is injected into the passage of valve in a conical shape. The direction of water spraying is opposite to the direction of steam flow, so as to the efficiency of heat transfer can be improved, and the flow length of cooling water in valve is extended. After the contact of cooling water and steam, they flow through the second and third orifice plates together. In this process, the cooling water will be evaporated by mixing with steam and absorbing heat, finally the steam temperature and pressure are reduced, which meet the requirement of supplying heat. The flow path of steam and water are shown in fig. 1. The extension sections are added at the model inlet and outlet to eliminate the influence caused by incomplete development of fluid-flow.

Evaporation model

When the cooling water contacts with high temperature steam, the sprayed cooling water will be evaporated due to the heating of high temperature steam, but the steam will be first condensed by releasing heat to water and then evaporated by absorbing the heat of high temperature steam at outer layer, which is a short process of phase transformation. In order to obtain a more practical process of temperature and pressure reduction, the transfer of energy and mass is considered in the calculation. The multiphase evaporation model in CFX is established to simulate the phase transformation of cooling water and steam. The specific mathematical process is as follows [26].

The boiling point of water is the function of evaporation pressure and temperature. According to the temperature, pressure and state coefficient of the steam, the boiling point is defined:

$$p_{\mathrm{v}} = p_{\mathrm{s}} \mathrm{e}^{a-b/(T_p+c)} \tag{1}$$

The boiling point of droplets consists of temperature and pressure, when the pressure of the mixture is higher than the pressure of boiling point, the droplets will evaporate into steam. While the pressure of the mixture is lower than the pressure of boiling point, the steam condenses into droplets. Similar to pressure boiling point, there is a temperature boiling point. When the droplets (cooling water) temperature is higher than the boiling point, the droplets will evaporate into steam. The mass transfer between steam and water in the process of evaporation is:

$$\frac{\mathrm{d}m_p}{\mathrm{d}t} = -\frac{Q_{\mathrm{C}} + Q_{\mathrm{R}}}{L} \tag{2}$$

The mass transfer between steam and water in the process of condensation is:

$$\frac{\mathrm{d}m_p}{\mathrm{d}t} = \pi d_p \rho D \mathrm{Sh} \frac{w_c}{w_g} \ln\left(\frac{1-x_{\mathrm{s}}^v}{1-x_{\mathrm{v}}^v}\right) \tag{3}$$

The continuous fluid mass source can be expressed:

$$\frac{\mathrm{d}m_p}{\mathrm{d}t} = \frac{\mathrm{d}S}{\mathrm{d}t} \tag{4}$$

The CFD simulations

According to the numerical simulation model established in [14, 15], the RNG k-ε turbulence model of CFX is selected to solve the 3-D flow field of MSHPTRV. The flow field is two-phase flow of steam and water, and the mixture of steam and water belongs to pure substance. So the governing equations of the flow field can be obtained as follows [26].

Mass conservation equation:

$$\frac{\partial \rho}{\partial t} + \mathrm{div}(\rho \vec{\mathrm{u}}) = 0 \tag{5}$$

Momentum conservation equation:

$$\frac{\partial(\rho u)}{\partial t}+\operatorname{div}(\rho u\vec{\mathrm{u}})=\operatorname{div}(\mu \operatorname{grad} u)-\frac{\partial p}{\partial x}+S_u \tag{6}$$

$$\frac{\partial(\rho v)}{\partial t}+\operatorname{div}(\rho v\vec{\mathrm{u}})=\operatorname{div}(\mu \operatorname{grad} v)-\frac{\partial p}{\partial y}+S_\mathrm{v} \tag{7}$$

$$\frac{\partial(\rho w)}{\partial t}+\operatorname{div}(\rho w\vec{\mathrm{u}})=\operatorname{div}(\mu \operatorname{grad} w)-\frac{\partial p}{\partial z}+S_w \tag{8}$$

The standard turbulent kinetic energy equation is as follows.
The k equation:

$$\frac{\partial(\rho k)}{\partial t}+\frac{\partial(\rho k u_i)}{\partial x_i}=\frac{\partial}{\partial x_j}\left[\left(\mu+\frac{\mu_t}{\sigma_k}\right)\frac{\partial k}{\partial x_j}\right]+G_k+G_b-\rho\varepsilon-Y_M+S_k \tag{9}$$

The ε equation:

$$\frac{\partial(\rho k)}{\partial t}+\frac{\partial(\rho\varepsilon u_i)}{\partial x_i}=\frac{\partial}{\partial x_j}\left[\left(\mu+\frac{\mu_t}{\sigma_\varepsilon}\right)\frac{\partial \varepsilon}{\partial x_j}\right]+C_{1\varepsilon}\frac{\varepsilon}{k}(G_k+C_{3\varepsilon}G_b)-C_{2\varepsilon}\rho\frac{\varepsilon^2}{k}+S_\varepsilon \tag{10}$$

The steam flow in MSHPTRV has the strong vortex motion. To solve the complex turbulent flow field accurately and present flow characteristics clearly, the RNG k-ε turbulence model is evolved by correcting the constants of standard k-ε model, in which the constant $C_{1\varepsilon}$ is replaced by the function $C_{1\varepsilon r}$:

$$C_{1\varepsilon r}=1.42-\frac{\left(\dfrac{P_k}{\rho C_{\mu r}}\right)^{1/2}\left[1-4.38^{-1}\left(\dfrac{P_k}{\rho C_{\mu r}}\right)^{1/2}\right]}{1+\beta_r\left(\dfrac{P_k}{\rho C_{\mu r}}\right)^{3/2}} \tag{11}$$

In the steady-state simulation, the boundary conditions of the numerical model are set as the rated working condition of MSHPTRV. The mass inlet and pressure outlet are adopted. The steam flow rate at the inlet of MSHPTRV is 91.67 kg/s and the steam temperature is 538 °C. The outlet pressure of MSHPTRV is 4.03 MPa, and the property of outlet boundary is set as *Opening* to adapt the backflow. The flow rate of spraying water is 14.45 kg/s and the cooling water comes from the outlet of feed pump. The cooling water temperature is 179 °C, the specific boundary conditions and parameters are shown in tab. 1. The convection and radiation are considered in the process of heat transfer, the dependent property of steam and water is adopted, so the water and steam can exchange heat according to different conditions of temperature and pressure. The transformation of heat and mass can be conducted according to eqs. (1)-(4).

The computational domain is constructed by computer aided design and the tetrahedral elements are generated to adapt complex geometry flexibly in ANSYS Meshing. The independence verification of mesh is carried out, and the suitable element number is determined, as shown in tab. 2. The results are reliable when the element number over 6 million. The minimum error of mass-flow rate is less than 0.002% when the element number over 8

Table. 1 Boundary conditions

Boundary	Value
Steam mass of inlet	91.67 kg/s
Steam pressure of outlet	4.03 MPa
Steam temperature of inlet	538 ℃
Flow rate of water	14.45 kg/s
Sprayed water temperature	179 ℃
Droplet diameter	0.001 mm
Initial velocity of droplets	60 m/s

Table. 2 Independent verification of mesh

Elements/10^4	294	417	639	818	928
Mass-flow rate [kgs^{-1}]	108.071	110.152	106.224	106.035	106.033
Error [%]	Min error = 0.002%				

million. Finally element number of 8 million is applied to flow field for tracking trajectory, the cells size between 0.02-1.0 mm and the mesh near the wall is refined. In order to obtain more accurate results, the convergent residuals of the equations reach 10^{-5}.

Experimental verification

The suitability of the RNG *k-ε* turbulence model for MSHPRV has been verified in [14, 15], but the evaporation model with water spraying is the first time to be used in the simulation of MSHPTRV, so it is necessary to verify the accuracy of evaporation model. Based on the original experimental platform of 50 kW steam turbine with oil burning boiler, fig. 2, the DN10 pressure and temperature reducing valve is installed in the bypass system. The installation of pressure and temperature reducing valve, as well as the measure points of temperature and pressure are shown in the fig. 3.

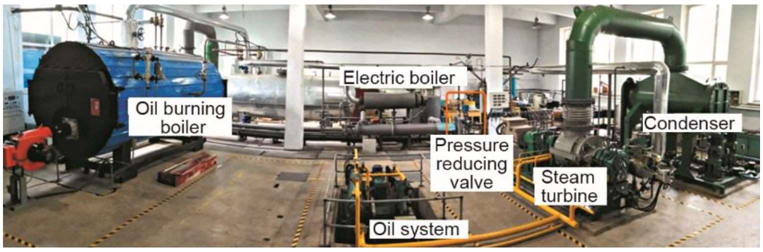

Figure 2. The 50 kW steam turbine with oil burning boiler

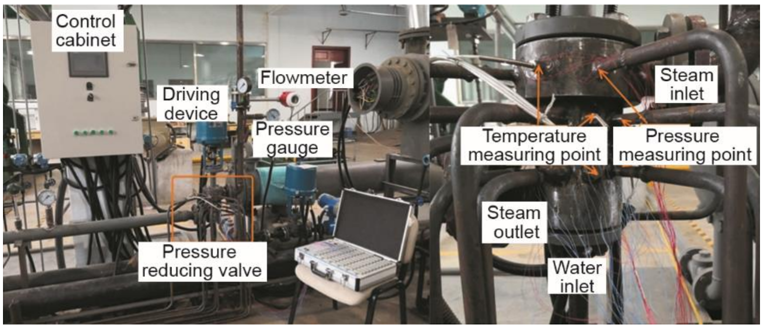

Figure 3. The MSHPTRV and measuring points

The oil burning boiler is used to heat water to produce steam, and the electric boiler can further heat the steam into superheated state. The designed steam temperature at the outlet of electric boiler is 165 ℃ and the outlet pressure is 0.6 MPa. Due to the heat dissipation of pipeline, the experimental temperature and pressure at the inlet of DN10 pressure and temperature reducing valve become 153 ℃ and 0.51 MPa, the temperature of the cooling water is 20 ℃. The designed steam temperature and pressure at the outlet of DN10 pressure and temperature reducing valve are 123 ℃ and 0.2 MPa. Finally, the outlet pressure and temperature of DN10 pressure and temperature reducing valve are 0.23 MPa and 132 ℃, respectively, the mass-flow of steam is 0.22 tonne per hours. According to the experimental parameters, the numerical simulation of DN10 pressure and temperature reducing valve is built, and the water spraying and evaporation model are adopted. The RNG k-ε turbulence model is also used in the calculation. The pressure and temperature ratio at the measure points relative to the inlet are shown in fig. 4.

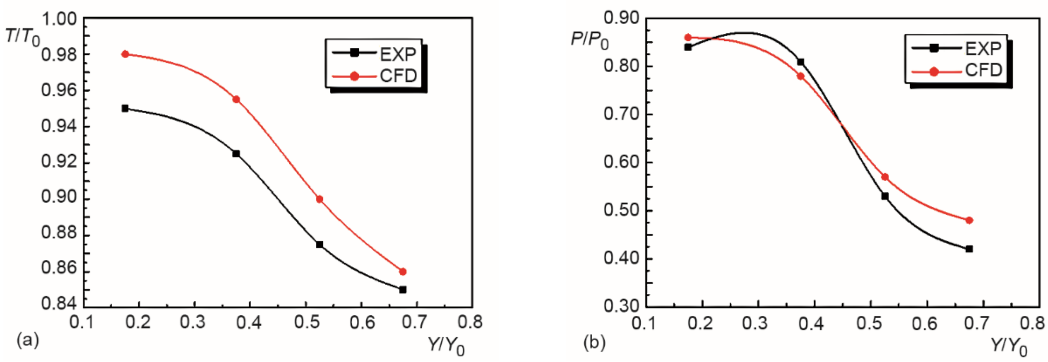

Figure 4. Pressure and temperature of experiment and numerical simulation; (a) temperature distribution in *y*-axis and (b) pressure distribution in *y*-axis

In order to obtain more accurate experimental data, the experiment is repeated three times to obtain the average value of the temperature and pressure. It can be shown that the experimental temperatures are lower than the simulation value due to the poor thermal insulation and thick valve body. But the variation of the temperature is similar. The evaporation process of sprayed water is considered in the experiment and compared with numerical simulation, which is the main purpose of the experiment. Although there are some errors between experiment and simulation, the similar variation of the indexes indicates that the evaporation model used in this study has a good effect.

Results and discussion

Figure 5 shows the pressure distributions in X-Y plane and cross-section. From the pressure distribution in X-Y plane, the steam pressure at downstream of first orifice plate is 13.6 MPa, the pressure difference between the upstream and downstream of first orifice plate is 2.8 MPa. The pressure is further reduced to 12.8 MPa between the first orifice plate and the water inlet. The pressure is slightly increased by the resistance effect of the wall near the water inlet. The steam pressure drop is 4.73 MPa when the steam flows through the second orifice plate. It is the maximum pressure drop among the pressure drops of three orifice plates, which accounts for 41.6% of the total pressure drop. This is because the flow passage near second orifice plate has the shape of gradual expansion which has the effect of pressure reducing, combined with the throttling of the orifice plate, the best pressure reducing effect is ultimately achieved. After the third orifice plate, the steam pressure in some areas is 3.36 MPa.

The final outlet pressure can be stable at 4.029 MPa in the extension section. From the pressure distribution in cross section, the distribution of pressure is more uniform in circumferential direction, and the inner-side pressure of second orifice plate is higher. The pressure at the inlet of orifice passage is low because of throttling effect.

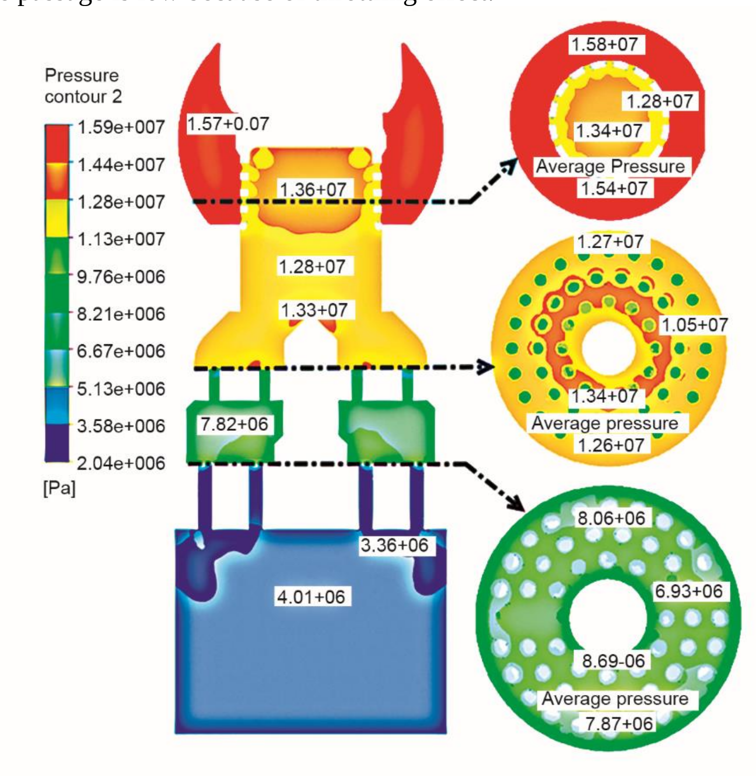

Figure 5. Pressure distribution

Figure 6 shows the temperature distribution in X-Y plane and cross-section. From the temperature distribution in X-Y plane, the steam temperature drops obviously in orifice passage when the steam flows through the first orifice. Since then, the steam temperature rises, because the steam velocity slow down and the kinetic energy is turned into heat energy. In the vicinity of water inlet, the steam contacts the cooling water, so the water absorbs the heat of steam and evaporates, which lead the rapid reduction of steam temperature. However, the steam temperature far away from the water inlet hardly changes. The mixing area of steam and water diffuses gradually by throttling and disturbance of second orifice plate. The steam and water are nearly fully mixed after third orifice plate, and the overall steam temperature has been reduced. It can be seen from the cross-section that the temperature distributions of the second and third orifice plate are uneven. The temperature of the second orifice plate has obvious stratification in the radial direction. The low temperature area at the middle of third orifice plate presents expansion, which indicates that the mixing degree of steam and cooling water is further improved. The large temperature difference of the second and third orifice plate caused by water spraying is a main reason for orifice plate stress. So the influence of temperature with water spraying should be considered in the fatigue analysis of MSHPTRV. This is what needs to be studied in the future.

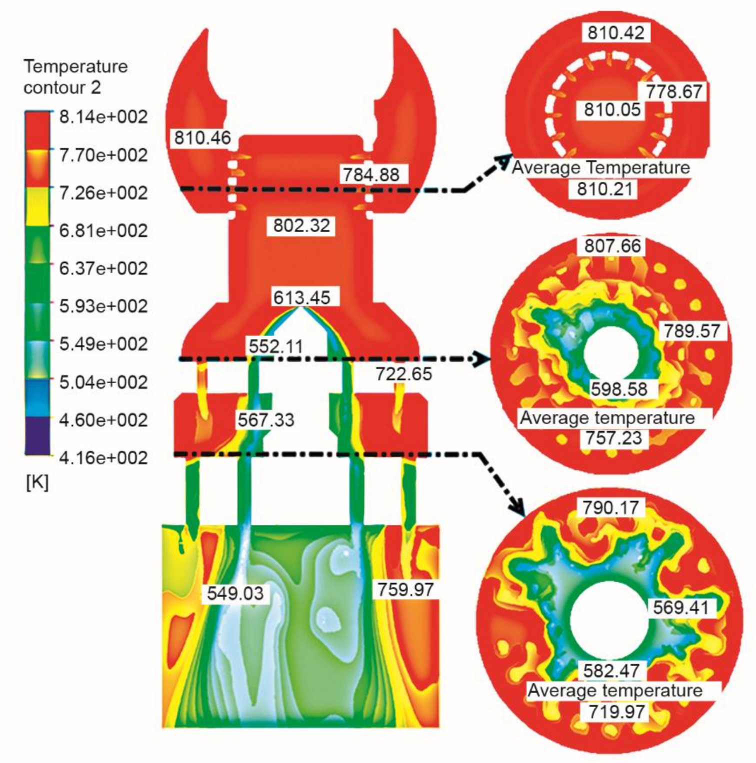

Figure 6. Temperature distribution

Figure 7 shows the streamlines of steam in MSHPTRV. The steam at the inlet of MSHPTRV is relatively uniform. At upstream of first orifice plate, the steam collides with the orifice plate and the most of steam accumulates to the back of valve core. There are many vortexes behind each orifice, which can produce large thermodynamic loss and reduce the temperature and pressure of steam. Between the upstream of second orifice plate and downstream of third orifice plate, the strong vortex motion is formed. So the most of kinetic energy is turned into the heat energy and absorbed by cooling water. The steam turbulence gradually decreases along the extension section and the steam flow near outlet is more orderly. Combined with flow field of water spraying in fig. 8, the water collides with the steam in convection, which formed a distinct layer *steam-water layer*. With the carrying effect of the steam, the droplets are accelerated, and the maximum velocity can exceed the local acoustic velocity. Therefore, it is necessary to consider the erosion damage of orifice plates caused by the incompletely evaporated droplets.

The working principle of MSHPTRV is converting high-quality energy into low--quality energy. The thermodynamic loss of MSHPTRV is great in essence, and the greater thermodynamic loss, the better effect of reducing pressure and temperature. Based on this theory, the efficient working area of MSHPTRV can be determined reversely by the distribution of thermodynamic loss.

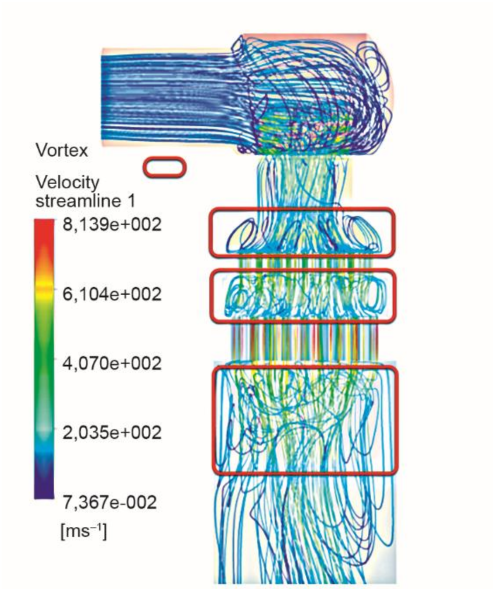

Figure 7. Streamline of MSHPTRV

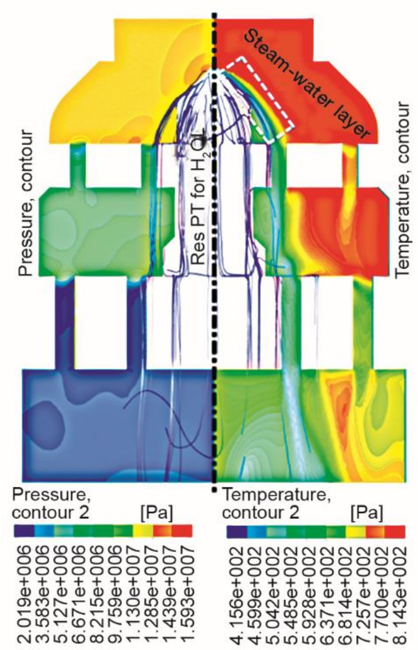

Figure 8. Flow field of water spraying

The increase rate of entropy S_{dis} can present the local loss of flow field, which relates to the steady-state conservation equation of entropy [27].

$$\iint_A \rho s\vec{u}\,\mathrm{d}A - \iint_A \frac{q_{\mathrm{in}}}{T}\mathrm{d}A = \iiint_V \dot{S}'''_{\mathrm{gen}}\mathrm{d}V \tag{12}$$

The increase rate of entropy is deducted by viscous loss $\dot{S}'''_{\mathrm{vsic}}$:

$$S_{\mathrm{dis}} = \frac{T_{t2}\dot{S}'''_{\mathrm{vsic}}}{\dfrac{1}{2}\left(\dfrac{\rho u^3}{h}\right)_{\mathrm{inlet}}} \tag{13}$$

$$\dot{S}'''_{\mathrm{vsic}} = \frac{\mu_{\mathrm{eff}}}{T}\left[\begin{aligned} &2\left(\frac{\partial u}{\partial x}\right)^2 + 2\left(\frac{\partial v}{\partial y}\right)^2 + 2\left(\frac{\partial w}{\partial z}\right)^2 + \left(\frac{\partial u}{\partial y} + \frac{\partial v}{\partial x}\right)^2 + \\ &+\left(\frac{\partial v}{\partial z} + \frac{\partial w}{\partial y}\right)^2 + \left(\frac{\partial w}{\partial x} + \frac{\partial u}{\partial z}\right)^2 - \frac{2}{3}\left(\frac{\partial u}{\partial x} + \frac{\partial v}{\partial y} + \frac{\partial w}{\partial z}\right)^2 \end{aligned}\right] \tag{14}$$

Increase rate of entropy S_{dis} in MSHPTRV is shown as fig. 9. The increase rate of entropy S_{dis} between upstream and downstream of orifice plates is great. The viscosity of steam is the one of main reasons for causing S_{dis}. The steam can be compressed and expanded in the progress of throttling, and the thermodynamic energy of steam will be converted into heat energy due to viscous friction, which reduces the quality of steam energy. In addition, the strong process of heat transfer will be acted when the water contacts with high temperature steam. Based on the Second law of thermodynamics, the process of heat transfer with large temperature difference can produce a lot of irreversible loss. The stronger the turbulence, the better the effect of heat transfer. This is why a large increase rate of entropy S_{dis} appears in the regions of steam-water mixing and strong turbulence. It can be seen from the contour of increase rate of entropy that S_{dis} can reach 0.053 at the outlet of the first orifice plate. The maximum S_{dis} is 0.782 at the inlet of the second orifice plate, and the S_{dis} at the outlet of second orifice plate is about 0.3. To clearly show the overall trend of thermodynamic loss in the process of steam flow, the average S_{dis} along the Y-co-ordinates is shown in fig. 10. The average S_{dis} between upstream and downstream of second orifice plate are great. Combined with pressure distribution, it is reasonable that the maximum loss and pressure drop both appear in the downstream of second orifice plate, which is the efficient working area of the MSHPTRV.

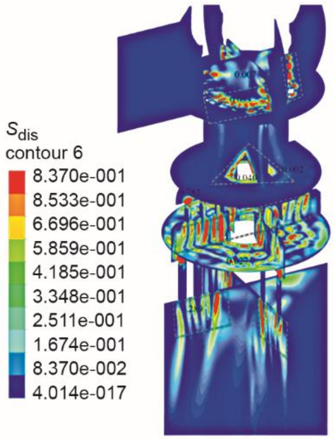

Figure 9. Increase rate of entropy S_{dis}

The working performance of the water spraying has a great influence on the effect of reducing temperature in MSHPTRV. The atomization effect of water spraying affects the length of evaporation section of the droplets. So the average volume fractions of the water under three different droplet diameters are calculated as shown in fig. 11.

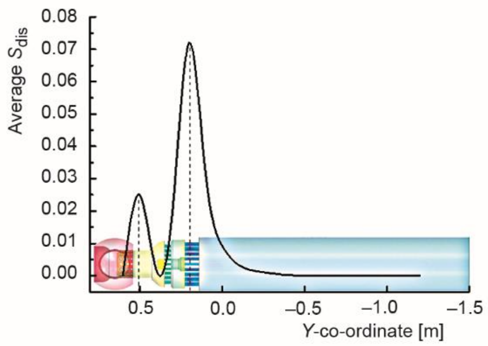

Figure 10. Average S_{dis} along Y-co-ordinate

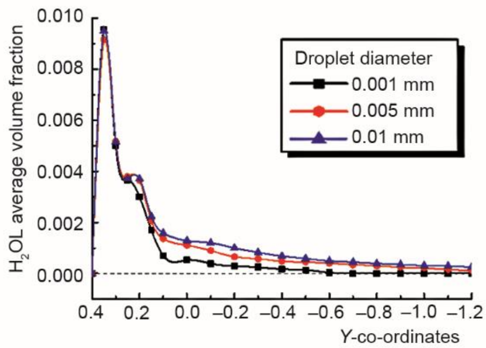

Figure 11. The H_2OL average volume fraction of three droplet diameters

At the upstream of the second orifice plate, the droplet diameter has little effect on the evaporation, while at the inlet and downstream of the second orifice plate, the droplet diameter seriously affects evaporation. This is because the steam temperature is enough high to heat the droplets when the water comes into the MSHPTRV. The droplets at the outside of steam-water layer have the strong evaporation capacity. So the droplets at the outside of steam-water layer can be completely evaporated no matter how large the diameter of the droplets. However, the heat absorption of the droplets at the inside of steam-water layer is limited and it is difficult to evaporate. In other words, at the upstream of the second orifice plate, the ability of steam heating droplets is strong, but the contact area of steam and droplets is limited, so the influence of droplet diameter is little. When the droplets reach the second orifice plate, the droplets at the inside of steam-water layer can be mixed with steam because the steam flow is disturbed by second orifice plate. The contact area of steam and droplets is increased, but the ability of steam heating droplets is limited because the steam temperature is low, so the small droplet diameter evaporates more easily, in which the influence of droplet diameter is prominent. When the droplet diameter is 0.001 mm, the length of evaporation section is only 0.6 m. However, the length of evaporation section for the droplet diameter 0.01 mm is over 2 m.

Conclusions

The water spraying and evaporation model verified by the experiment are integrated into the MSHPTRV. On this basis, the thermodynamic loss and efficient working area of MSHPTRV are analyzed. The influence of droplet diameter on the evaporation section is studied. The specific conclusions are as follows.

- The water spraying and evaporation model integrated into MSHPTRV have the good agreement with the experiment. The thermodynamic process of 200 ℃ temperature difference and 11.3 MPa pressure drop in bypass heating system can be achieved by the MSHPTRV. The three-stage pressure drops, respectively, account for 24.6%, 41.6%, and 33.8% of the total pressure drop.
- The vortexes and evaporation of water can produce thermodynamic loss and reduce the steam temperature and pressure. A distinct layer *steam-water layer* is formed at the mixing area of water and steam. The temperature distributions of the second and third orifice plate are uneven.
- The increase rate of entropy S_{dis} at the water inlet, upstream and downstream of orifice plates are great, where the thermodynamic loss is also great. The maximum S_{dis} is 0.782 at the inlet of the second orifice plate. The downstream of second orifice plates is the efficient working area of MSHPTRV.
- The droplet diameter has little effect on the evaporation at the upstream of the second orifice plate, but seriously affects evaporation at the downstream of the second orifice. The length of evaporation section increases with the droplet diameter.

Acknowledgment

The authors would like to give their acknowledgement to National Key R&D Plan (2017YFB0902100) for the financial support on the paper.

Nomenclature

a – state coefficient (selected by the steam properties)
b – steam enthalpy coefficient (selected by the steam properties)
$C_{1\varepsilon}$ – empirical value (= 1.44)
$C_{2\varepsilon}$ – empirical value, (= 1.92)
$C_{3\varepsilon}$ – empirical value (determined by k and ε)
$C_{\mu r}$ – RNG k–ε turbulence model constant, (= 0.085)
c – steam temperature coefficient (selected by the steam properties)
d_p – droplet diameter, [m]
G_b – generation terms of turbulent kinetic energy, k (caused by buoyancy)
G_{k} – generation terms of turbulent kinetic energy k (caused by average velocity gradient)
L – latent heat of vaporization, [Jkg^{-1}]
m_{p} – droplet mass, [kg]
P_k – shear production of turbulence, [Pa·s]
p_{s} – steam pressure, [Pa]
Q_{C} – convective heat, [J]
Q_{R} – radiant heat, [J]
q_{in} – heat of control body, [Jm^{-2}]
S – mass source, [kg]
Sh – Sherwood coefficient (determined by droplet size and properties)
S_k – source items (corresponding to the turbulent kinetic energy, k)

S_u – generalized source terms of *x*-direction
S_v – generalized source terms of *y*-direction
S_w – generalized source terms of *z*-direction
S_ε – source items (corresponding to the dissipation rate, ε)
T_p – steam temperature, [°C]
t – time, [s]
$\vec{u}$ – velocity vector
u – velocity of *x*-direction, [ms^{-1}]
u_i – mean velocity, [ms^{-1}]
v – velocity of *y*-direction, [ms^{-1}]
V – volume, [m^3]
w – velocity, [ms^{-1}]
w_c – steam molecular weight
w_g – mixture molecular weight
x_s^v – vapor mole fraction
x_v^v – mixture gas mole fraction
Y_M – expansion of pulsation in compressible turbulence

Greek symbols

β_r – RNG k-ε turbulence model constant, (= 0.012)
μ – dynamic viscosity, [Nsm^{-2}]
μ_t – eddy viscosity, [Nsm^{-2}]
μ_eff – effective viscosity coefficient, [Pa·s]
ρ – fluid density, [kgm^{-3}]
ρD – dynamic diffusion coefficient
σ_k – Prandtl number (corresponding to the turbulent kinetic energy, k)
σ_ε – Prandtl number (corresponding to the dissipation rate, ε)

Acronyms

MSHPTRV – multi-stage high pressure and temperature reducing valve
MSHPRV – multi-stage high pressure reducing valve

References

[1] Zou, D., *et al.*, Solving the Combined Heat and Power Economic Dispatch Problems by an Improved Genetic Algorithm and a New Constraint Handling Strategy, *Appled Energy, 237* (2019), Mar., pp. 646-670
[2] Pujihatma, P., *et al.*, Combined Heat and Power – Multi-Objective Optimization with an Associated Petroleum and wet Gas Utilization Constraint, *Journal of Natural Gas ence and Engineering, 54* (2018), June, pp. 25-36
[3] Wu, M. Q., Comparison of Integrated and Divided Desuperheater (in Chinese), *Chemical Engineering Design Communications, 42* (2016), 2, pp. 101-107
[4] Li, G., *et al.*, The Structure Design and Analysis of Temperature and Pressure of Water Cooling (in Chinese), *Valve*, (2015) 4, pp. 7-9
[5] Wang, P., *et al.*, Influence of a Circular Strainer on Unsteady Flow Behavior in Steam Turbine Control Valves, *Applied Thermal Engineering, 115* (2017), Mar., pp. 463-476
[6] Wang, P., *et al.*, Unsteady Flow Behavior of a Steam Turbine Control Valve in the Choked Condition: Field Measurement, Detached Eddy Simulation and Acoustic Modal Analysis, *Applied Thermal Engineering, 117* (2017), May, pp. 725-739
[7] Zhao, B., *et al.*, FSI Model of Valve Motion and Pressure Pulsation for Investigating Thermodynamic Process and Internal Flow Inside a Reciprocating Compressor, *Applied Thermal Engineering, 131* (2018), Feb., pp. 998-1007
[8] Fan, X., *et al.*, Energy Consumption Investigation of Electromagnetic Valve Train at Gas Pressure Conditions, *Applied Thermal Engineering, 146* (2019), Jan., pp. 768-774
[9] Qian, J. Y., *et al.*, Mach Number Analysis on Multi-Stage Perforated Plates in High Pressure Reducing Valve, *Energy Conversion & Management, 119* (2016), July, pp. 81-90
[10] Qian, J. Y., *et al.*, Flow Rate Analysis of Compressible Superheated Steam Through Pressure Reducing Valves, *Energy, 135* (2017), Sept., pp. 650-658
[11] Xu, H., *et al.*, Hydrodynamic Characterization and Optimization of Contra-Push Check Valve by Numerical Simulation, *Annals of Nuclear Energy, 38* (2011), 6, pp. 1427-1437
[12] Li, S., *et al.*, CFD Simulation of Dynamic Characteristics of a Solenoid Valve for Exhaust Gas Turbocharger System, *Applied Thermal Engineering, 110* (2017), Jan., pp. 213-222
[13] Jin, Z. J., *et al.*, Numerical Analysis of Flow and Temperature Characteristics in a High Multi-Stage Pressure Reducing Valve for Hydrogen Refueling Station, *International Journal of Hydrogen Energy, 41* (2016), 12, pp. 5559-5570
[14] Zhang, J., *et al.*, Prediction of Blowdown of a Pressure Relief Valve Using Response Surface Methodology and CFD Techniques, *Applied Thermal Engineering, 133* (2018), Mar., pp. 713-726
[15] Hou, C. W., *et al.*, Parametric Analysis on Throttling Components of Multi-Stage High Pressure Reducing Valve, *Applied Thermal Engineering, 128* (2018), Jan., pp. 1238-1248

[16] Aung, N. Z., *et al.*, CFD Analysis of Flow Forces and Energy Loss Characteristics in a Flapper-Nozzle Pilot Valve with Different Null Clearances, *Energy Conversion & Management, 83* (2014), July, pp. 284-295
[17] Menendez, B., *et al.*, Unsteady Three-Dimensional Modeling of the Fluid-Structure Interaction in the Check Valves of Diaphragm Volumetric Pumps, *Journal of Fluids and Structures, 90* (2019), Oct., pp. 432-449
[18] Li, F., Q, *et al.*, Transient Thermal Behaviors of a Scaled Turbine Valve: Conjugate Heat Transfer Simulation and Experimental Measurement, *International Journal of Heat and Mass Transfer, 141* (2019), Oct., pp. 116-128
[19] Jalali, A., *et al.*, Failure Analysis in a Steam Turbine Stop Valve of a Thermal Power Plant, *Engineering Failure Analysis, 105* (2019), Nov., pp. 1131-1140
[20] Chen, F. Q., *et al.*, Pressure Analysis on Two-Step High Pressure Reducing System for Hydrogen Fuel Cell Electric Vehicle, *International Journal of Hydrogen Energy, 42* (2017), 16, pp. 11541-11552
[21] Chen, F. Q., *et al.*, Turbulent Compressible Flow Analysis on Multi-Stage High Pressure Reducing Valve, Flow *Measurement and Instrumentation, 61* (2018), June, pp. 26-37
[22] Chen, F. Q., *et al.*, Thermo-Mechanical Stress and Fatigue Damage Analysis on Multi-Stage High Pressure Reducing Valve, *Annals of Nuclear Energy, 110* (2017), Dec., pp. 753-767
[23] Boccardi, G., *et al.*, Two-Phase Flow Through Pressure Safety Valves. Experimental Investigation and Model Prediction, *Chemical Engineering Science, 60* (2005), 19, pp. 5284-5293
[24] Schmidt, J., Sizing of Nozzles, Venturis, Orifices, Control and Safety Valves for Initially Sub-Cooled Gas/Liquid Two-Phase Flow – The HNE-DS Method, *Forschung Im Ingenieurwesen, 71* (2007), 47, pp. 47-58
[25] Mansour, A., *et al.*, A Review of Flash Evaporation Phenomena and Resulting Shock Waves, *Experimental Thermal and Fluid Science, 107* (2019), Oct., pp. 146-168
[26] Xu, M., *et al.*, Effect of Water Spray in Exhaust Passage of Steam Turbine on Flow Field of the Last Stage During Windage, *International Journal of Heat and Mass Transfer, 161* (2020), Nov., pp. 120296
[27] Cao, L., *et al.*, Effects of Leakage Vortex on Aerodynamic Performance and Loss Mechanism of Steam Turbine, *Proceedings of the Institution of Mechanical Engineers Part A Journal of Power and Energy, 233* (2019), 7, pp. 866-876

Paper submitted: July 19, 2020
Paper revised: March 2, 2021
Paper accepted: March 9, 2021